WATER RESOURCES RESEARCH, VOL. 30, NO. 5, PAGES 1571–1587, MAY 1994

Interpretation of isotopic data in groundwater-rock systems: Model development and application to Sr isotope data from Yucca Mountain

Thomas M. Johnson and Donald J. DePaolo

Berkeley Center for Isotope Geochemistry, Department of Geology and Geophysics, University of California, Berkeley
Earth Sciences Division, Lawrence Berkeley Laboratory, Berkeley, California

Abstract. A model enabling extraction of hydrologic information from spatial and temporal patterns in measurements of isotope ratios in water-rock systems is presented. The model describes the evolution of isotope ratios in response to solute transport and water-rock interaction. In advective systems, a single dimensionless parameter (a Damköhler number, N_D) dominates in determining the distance over which isotopic equilibrium between the water and rock is approached. Some isotope ratios act as conservative tracers ($N_D \ll 1$), while others reflect only interaction with the local host rock ($N_D \gg 1$). If N_D is close to one (i.e., the distance for equilibration is close to the length scale of observation), isotope ratio measurements can be used to determine N_D, which in turn may yield information concerning reaction rates, or spatial variations in water velocity. Zones of high velocity (e.g., as a result of greater fracture density), or less reactive zones, may be identified through observation of their lower N_D values. The model is applied to paleohydrologic interpretations of Sr isotope data from calcite fracture fillings in drill cores from Yucca Mountain, Nevada (Marshall et al., 1992). The results agree with other studies suggesting "fast path" transport in the unsaturated zone. Also, we find that the data do not give a conclusive indication of paleowater table elevation because of the effects of water-rock interaction.

Introduction

Isotopic measurements are increasingly used for hydrologic characterization in groundwater systems. Values of $\delta^{18}O$ and δD vary with time and space in the precipitation at recharge areas, and the isotope ratios of dissolved elements (e.g., Sr, C, Nd, Pb, U, S) are influenced by the soil and rock the waters pass through. The resulting isotopic contrasts give rise to spatial and/or temporal patterns in isotope ratios that contain information about flow paths, water-rock interaction, and mixing relationships. This approach has been used in hydrologic studies from the catchment scale [e.g., *Sklash*, 1990; *McDonnell et al.*, 1990; *Kennedy et al.*, 1986; *Bullen and Kendall*, 1991] to regional scale [e.g., *Banner et al.*, 1989; *Musgrove and Banner*, 1993; *Stueber et al.*, 1993; *Peterman and Stuckless*, 1993; *Ludwig et al.*, 1993; *Stuckless et al.*, 1991; *McNutt et al.*, 1987].

When information is desired regarding the past properties of a hydrologic system, physical prediction of water flow is impossible and the information recorded in minerals deposited in past regimes is of great value [*Bottomley and Veizer*, 1992; *Marshall et al.*, 1992; *Paces et al.*, 1993; *Whelan and Stuckless*, 1992; *Quade and Cerling*, 1990; *Shemesh et al.*, 1992]. Among the various chemical measurements that can be performed on these minerals, isotope ratio measurements are among the most easily interpreted, because of the simplicity of the equilibrium condition. Effectively, the isotope ratios of Sr, Nd, Pb, and other "nonfractionating" elements in solution-deposited minerals are always equal to those of the parent water (slight fractionations do occur, but these are canceled during the analysis process); thus these isotope ratios directly record water conditions at the time of precipitation, with possible alteration due to subsequent cation exchange. The isotope ratios of O, C, H, and other lighter elements record the isotope ratios of the parent fluid, modified by temperature-dependent fractionation. Measurements of all of the isotope ratios are extremely precise, enabling detection of small variations in paleohydrologic conditions.

Isotope measurements, either on sampled groundwater or on water-deposited minerals, yield spatial or temporal patterns that contain information concerning groundwater flow and transport conditions. One is then faced with an inverse problem: to extract information about the physical processes that govern groundwater flow and/or the chemical processes that govern the evolution of isotope ratios along the fluid flow path, from the observed compositions created by these processes. In some systems, certain isotope ratios provide conservative tracers influenced only by the physical processes of fluid flow. For example, distinct hydrogen isotope ratios in separate recharge areas in a groundwater basin may serve to mark the paths of water masses through the basin. In other cases the chemical interaction of water and rock strongly influences the isotopic composition of the water. The latter case is common despite the slow reaction rates in low-temperature systems, because the concentration of most chemical elements of interest in isotope studies is orders of

Paper number 94WR00157.
0043-1397/94/94WR-00157$05.00

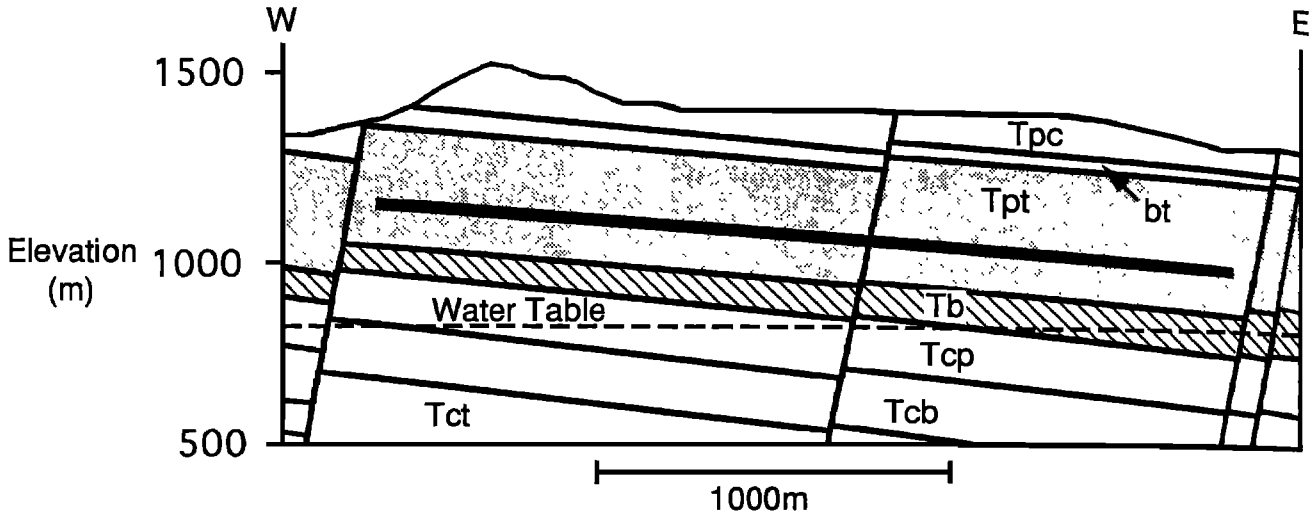

Figure 1. Simplified geologic cross section of Yucca Mountain [after *Sinnock et al.*, 1987]. The stratigraphy consist of a series of silicic tuffs labeled as follows: Tpc denotes Tiva Canyon member of the Paintbrush tuff; bt denotes unnamed bedded tuff; Tpt (stippled) denotes Topopah Springs member of the Paintbrush tuff; Tb (hatched) denotes tuffaceous beds of Calico Hills; Tcp, Tcb, Tct denote Prow Pass, Bullfrog, and Tram members of the Crater Flat tuff, respectively. The tentative repository zone is shown in heavy stippling.

magnitude greater in the solid phases than in the fluid. This work attempts to better systematize the application of isotope ratio variations in hydrology by providing a model that relates isotopic data in water-rock systems to the transport parameters of the systems, with emphasis on the influence of water-rock interaction. Ideally, this model could be used to extract solute transport parameters in undisturbed natural systems at the field scale; this would be of special interest in fractured rock or unsaturated flow regimes where it is very difficult to predict solute migration using physically based models.

An application of the model is presented, using data from the proposed nuclear waste repository site at Yucca Mountain, Nevada. Isotopic measurements on secondary minerals [*Marshall et al.*, 1992] provide information regarding the paleohydrology, and these data are interpreted through construction of models of the chemical evolution of groundwater flowing through the silicic tuff units at the site. The paleohydrologic record is of great concern at Yucca Mountain, because the safety of the proposed nuclear waste repository depends on the existence over many thousands of years of a thick unsaturated zone (Figure 1) where groundwater transport is predicted to be very slow [*Winograd*, 1974; *Sinnock et al.*, 1987]. Various scenarios for the paleohydrology of Yucca Mountain have been discussed [*National Research Council*, 1992], including higher water table conditions and active upwelling of water, and we discuss whether or not these models are consistent with available data on the Sr isotope composition of vein-filling calcite from deep boreholes.

Transport-Reaction Model for Isotope Ratios in Water-Rock Systems

The notation employed below is summarized at the end of the paper. The model constructed here relates the isotope ratios in the fluid as a function of position and time to the processes of reaction between fluid and rock and transport by advection and dispersion in a porous medium. The combined effects of three-dimensional transport and reaction on the concentration of dissolved species can be expressed

$$\frac{\partial c_f}{\partial t} = \nabla \cdot (\mathbf{D}\nabla c_f) - \mathbf{v} \cdot \nabla c_f + \sum_{i=1}^{n} J_i \qquad (1)$$

where c_f is the concentration of the species in the fluid at a given time and position, v is the average fluid velocity, D is the dispersion matrix, and J_i is the "reaction flux," the mass of the species delivered by a particular reaction to a unit volume fluid per unit time (precipitation gives negative values). Expressions of (1) for two isotopes of a chemical element can be combined to yield an expression for the isotope ratio:

$$\frac{\partial r_f}{\partial t} = \nabla \cdot (\mathbf{D}\nabla r_f) + \frac{2\mathbf{D}}{c_{2,f}} \nabla c_{2,f} \cdot \nabla r_f - \mathbf{v} \cdot \nabla r_f + \sum_{i=1}^{n} \frac{J_{2,i}}{c_{2,f}} [r_i - r_f] \qquad (2)$$

where r_f and r_i are the isotope ratios in the fluid and in the reaction products, respectively, $J_{2,i}$ is the reaction flux of the isotope in the denominator of the isotope ratio (e.g., ^{86}Sr), and $c_{2,f}$ is the concentration of the denominator isotope in the fluid phase. For most isotope pairs the following approximations are convenient, allowing one to use normal concentration values:

$$\frac{1}{c_{2,f}} \nabla c_{2,f} \approx \frac{1}{c_f} \nabla c_f \qquad (3)$$

$$\frac{J_{2,i}}{c_{2,f}} \approx \frac{J_i}{c_f} \qquad (4)$$

Because the abundance of the denominator isotope as a fraction of the total elemental abundance generally varies little (usually, $c_{2,f} \gg c_{1,f}$ and $J_{2,f} \gg J_{1,f}$), these approximations usually introduce negligible error (<1%). A notable exception is Pb isotopes, where the error may be of the order of 10%. Substituting (3) and (4) into (2) gives

$$\frac{\partial r_f}{\partial t} = \nabla \cdot (\mathbf{D}\nabla r_f) + \frac{2\mathbf{D}}{c_f} \nabla c_f \cdot \nabla r_f - \mathbf{v} \cdot \nabla r_f + \sum_{i=1}^{n} \frac{J_i}{c_f} [r_i - r_f] \quad (5)$$

Dissolution/Precipitation Reactions

The reaction fluxes J_i can be produced by dissolution of rock, precipitation of minerals, and/or ion exchange/sorption. In low-temperature groundwater systems, these processes proceed relatively slowly, and the fluid is often far from isotopic equilibrium with the solid phases. Accordingly, the approach adopted here is to treat the reaction rates as parameters of the system that may be either specified or solved for as unknowns. Predictions of reaction rates based on kinetic theory are commonly carried out and can be used if they are available. Adopting this treatment of reaction rates, dissolution and precipitation fluxes can be expressed

$$J_i = MR_iW_ic_i \quad (6)$$

R_i is the reaction rate of the ith reaction, expressed as the fractional decrease in the mass of reactant per unit time. Dissolution is represented by positive reaction rates, while precipitation results in negative rates. W_i is the mass fraction of the reactant in the rock, c_i is the concentration of the element of interest in the reacting phase, and M is the solid-to-fluid mass ratio:

$$M = \frac{(1 - \phi)\rho_s}{\phi \rho_f S_w} \quad (7)$$

where ϕ is the porosity, ρ_s is the solid density, and ρ_f is the fluid density. S_w is the saturation ratio (fraction of void space occupied by fluid). This particular form is utilized here because it enables the use of geologically observed reaction rates (e.g., it might be observed that 2% of a limestone unit was dissolved over 10 million years). The reaction fluxes can also be broken down according to surface area rather than mass, as would be preferable if kinetic information is to be incorporated into the model. In fact, in the case of sorption reactions, this alternate formulation is required. Regardless of the particular form used, the reaction flux depends on the concentration of the chemical element of interest in the reacting solid phase and the amount of reacting solid relative to the amount of fluid per unit volume. Substituting (6) into (5) yields

$$\frac{\partial r_f}{\partial t} = \nabla \cdot (\mathbf{D}\nabla r_f) + \frac{2\mathbf{D}}{c_f} \nabla c_f \cdot \nabla r_f - \mathbf{v} \cdot \nabla r_f + M \sum_{i=1}^{n} \frac{R_iW_ic_i}{c_f} [r_i - r_f] \quad (8)$$

For nonfractionating isotopes, precipitation reactions do not affect the isotopic composition of the fluid directly, so they do not appear in (8); however, they do affect c_f, and this may be considered separately if necessary.

For fractionating isotopes, delta notation is used in place of isotope ratios, and the reaction terms for dissolution and precipitation reactions differ in form. For dissolution the solid phase is transferred to the fluid in bulk (i.e., no fractionation occurs), so the reaction term in (8) applies. However, the isotope ratios of precipitated phases are not equal to that of the fluid. Assuming these phases are in isotopic equilibrium with the fluid, r_i in (8) must be replaced with $\alpha_j r_f$, where j is the index for precipitation reactions and α_j is the equilibrium fractionation factor for a precipitating phase at the temperature of interest:

$$\alpha_j(T) = (r_j/r_f)_{\text{equilib.}} \quad (9)$$

Isotope ratios of the fractionating type are commonly represented using delta notation, which gives the per mil deviation of the ratio from a standard ratio:

$$\delta = \frac{r - r_{\text{std}}}{r_{\text{std}}} \times 1000 \quad (10)$$

Converting (8) to δ notation and creating a new reaction term for the precipitation reactions gives

$$\frac{\partial \delta_f}{\partial t} = \nabla \cdot (\mathbf{D}\nabla \delta_f) + \frac{2\mathbf{D}}{c_f} \nabla c_f \cdot \nabla \delta_f - \mathbf{v} \cdot \nabla \delta_f + M \sum_{i=1}^{n} \frac{R_iW_ic_i}{c_f} [\delta_i - \delta_f] + M \sum_{j=1}^{n} \frac{R_jW_jc_j}{c_f} [\Delta_j(T)] \quad (11)$$

where Δ_j is the equilibrium difference between the δ values of the fluid and a precipitating phase:

$$\Delta_j(T) \equiv (\delta_j - \delta_f)_{\text{equilib.}} \quad (12)$$

The reader will note that for $\Delta_j = 0$ (i.e., $\alpha_j = 1$), (11) reduces to the same form as (8), with the only difference being the substitution of r for δ. The reaction term is equivalent to that of *Wigley et al.* [1978], though the form is very different.

Equation (8) for nonfractionating isotopes, or (11) for fractionating isotopes, relates the isotopic composition of the fluid, as a function of time and position, to the transport parameters $\mathbf{D}(\mathbf{x})$ and $\mathbf{v}(\mathbf{x})$, the reaction rates $R_i(\mathbf{x})$, and other parameters $r_i(\mathbf{x})$, $M(\mathbf{x})$, $c_i(\mathbf{x})$, and $c_f(\mathbf{x})$. The reader will note that in this three-dimensional formulation, mixing effects are included via the transverse dispersion terms in the dispersion matrix. Thus this differential equation describes the effects of translation of fluid, dispersion in the direction of flow, mixing between adjacent, distinct water masses, and interaction between water and rock or soil on the isotopic composition of the water. It provides the framework through which the isotope ratios measured in the fluid may be quantitatively interpreted. As shown below, the form used for the reaction terms can be applied to ion exchange in addition to dissolution and precipitation, so the model is widely applicable.

Mathematically, (8) and (11) share the same form, and the reader will note that it is similar to the form of the transport-

reaction equation for solute concentrations except for two items. First, the reaction terms in (8) and (11) contain r_f and δ_f, respectively; this gives rise to exponential solutions to the equations. Second, an additional dispersion term exists in the isotope expressions. This term can be important, especially if sharp gradients in concentration of the chemical element of interest are modeled. In the case where concentration variations are small, the term can be neglected.

Exchange and Sorption Reactions

Exchange reactions are modeled here with the same mathematics as dissolution and precipitation. The exchange process can be conceptualized as fluxes passing from the mineral to the fluid and vice versa. For nonfractionating isotopes, the process is simple: The flux passing to the mineral has the same isotopic ratio as the fluid, so it does not appear in the expression, as with the precipitation reactions. The flux diffusing into the fluid from the mineral has the isotope ratio of the mineral, r_i. The expression is thus the same as for a dissolution reaction, except in this case the reaction rate, R_i, represents the fraction of the ion of interest exchanged per unit time. If a fractionating isotope pair is to be considered in an exchange reaction, the situation is more complex. As a first-order approximation, (11) is used to represent the fluxes into and out of the mineral, with the same reaction rate used in both flux terms. This approach has also been used by *Criss et al.* [1987], *Lassey and Blattner* [1988], and *Blattner and Lassey* [1989]. Sorption onto surfaces is considered here to operate in a manner similar to lattice-site exchange reactions (e.g., zeolite cation exchange), and the atoms adsorbed onto surfaces are treated as a distinct solid "phase." In this case, the W_i and M parameters are modified to consider surface area instead of mass.

Evolution of Isotope Ratios in Solid Phases

In many cases the solid phases evolve much more slowly than the timescale of observation and can be considered fixed in composition. In low-temperature systems the compositions and modal abundances of most minerals are not significantly affected by the sluggish reactions on the timescale over which the fluid evolves. This does not mean that the fluid is not affected greatly by the reactions, however. The concentrations of many elements are orders of magnitude smaller in the fluid than in the solid phases, so a small amount of reaction produces a large flux from the solid relative to the concentration in the fluid.

In higher-temperature systems, or in the case of adsorption or rapid cation exchange in low-temperature systems, the solid phases cannot be considered invariant. For dissolution reactions the composition of the solid remains fixed while its abundance decreases (and ϕ decreases as well). For precipitation, exchange, or sorption reactions the evolution of an isotope ratio of each of the solid phases can be expressed

$$\frac{\partial r_i}{\partial t} = -R_i[r_i - \alpha_i r_f] \tag{13}$$

In a system where the solid phases change substantially, statements of (13), which describe the evolution of the solid phases, must be solved simultaneously with (8) or (11) in order to accurately describe the system [e.g., *Richter and DePaolo*, 1987, 1988; *Schrag et al.*, 1992].

Combined Reaction Term Form

The terms for the individual solid phases can be combined into a single term for the total flux from or to the reacting solid phases. In the discussion that follows, the fluxes to and from the solid phases are described as precipitation and dissolution fluxes for clarity, but the mathematics apply for exchange reactions also, as described above. With the reaction terms combined, (8) can be expressed

$$\frac{\partial r_f}{\partial t} = \nabla \cdot (\mathbf{D}\nabla r_f) + \frac{2\mathbf{D}}{c_f}\nabla c_f \cdot \nabla r_f - \mathbf{v} \cdot \nabla r_f + \bar{R}_d M \frac{c_s}{c_f}[\bar{r}_d - r_f] \tag{14}$$

where $\bar{r}_d$ is the isotope ratio of the total dissolution flux from the solid,

$$\bar{r}_d = \frac{\sum_{i=1}^{n} R_i W_i c_i r_i}{\sum_{i=1}^{n} R_i W_i c_i} \tag{15}$$

c_s is the concentration of the element in the whole rock, and $\bar{R}_d$ is the weighted sum of the individual dissolution rates:

$$\bar{R}_d = \sum_{i=1}^{n} R_i \frac{W_i c_i}{c_s} \tag{16}$$

Equation (11) can be manipulated in the same way, and the dissolution and precipitation terms combined to yield

$$\frac{\partial \delta_f}{\partial t} = \nabla \cdot (\mathbf{D}\nabla \delta_f) + \frac{2\mathbf{D}}{c_f}\nabla c_f \cdot \nabla \delta_f - \mathbf{v} \cdot \nabla \delta_f + \bar{R}_d M \frac{c_s}{c_f}\left[\bar{\delta}_d - \delta_f + \frac{\bar{R}_p}{\bar{R}_d}\bar{\Delta}\right] \tag{17}$$

where $\bar{\delta}_d$ is the value for the combined dissolution flux, $\bar{R}_p$ is a summed precipitation rate similar to $\bar{R}_d$, and $\bar{\Delta}$ is the flux-weighted mean for the fractionation constants:

$$\bar{\Delta} = \frac{\sum_{j=1}^{n} R_j W_j c_j \Delta_j}{\sum_{j=1}^{n} R_j W_j c_j} \tag{18}$$

Equations (14) and (17) give a convenient means of expressing the reaction terms as a single combined term that expresses the total effect of all the reactions without specifying the individual reaction rates. This is useful both as a compact notation (used in the discussion below) and when whole rock isotope ratios are used as an approximation for the isotope ratio of the reaction flux.

The Damköhler Number for Advective Systems

In advective water-rock or water-soil systems the spatial patterns observed in isotope measurements are related to two processes: First, the mixing of isotopically distinct fluid masses leads to spatial gradients that can be related to the rate of dispersive action. This effect is accounted for in the dispersion terms of the above equations. Second, reactions between the fluid and the solid phases alter the isotopic composition of the fluid, and the distance over which this occurs depends on the relative rates of advection and reaction. The central theme of this paper is to examine this second effect. In this section we illustrate the effects of coupled reaction and transport using a one-dimensional model, with x representing distance traveled along a flow path. This assumes that there is no net transport in the other dimensions (i.e., no mixing of distinct fluid masses); mixing effects are neglected to demonstrate the reaction effects. Also, for simplicity, the fluid velocity and dispersion coefficient are held constant over distance.

Working first with the equation for nonfractionating isotopes, (14) can be scaled by performing two substitutions. The distance variable can be scaled relative to some characteristic length of the system, ℓ:

$$x' = x/\ell \tag{19}$$

For advective systems it is useful to replace t with a dimensionless time, t':

$$t' = tv/\ell \tag{20}$$

After the substitutions and conversion to one dimension, (14) can be rearranged to yield

$$\frac{\partial r_f}{\partial t'} = \frac{D}{v\ell}\frac{\partial^2 r_f}{\partial x'^2} + \frac{2D}{v\ell c_f}\frac{\partial c_f}{\partial x'}\frac{\partial r_f}{\partial x'} - \frac{\partial r_f}{\partial x'} + \frac{\ell M \bar{R}_d c_s}{v c_f}[\bar{r}_d - r_f]$$

$$= \frac{1}{Pe}\left(\frac{\partial^2 r_f}{\partial x'^2} + \frac{2}{c_f}\frac{\partial c_f}{\partial x'}\frac{\partial r_f}{\partial x'}\right) - \frac{\partial r_f}{\partial x'} + N_D[\bar{r}_d - r_f] \tag{21}$$

where Pe is a Péclet number and N_D is a Damköhler number [*Lassey and Blattner*, 1988; *Blattner and Lassey*, 1989; *Boucher and Alves*, 1959], a dimensionless quantity that expresses the ratio of the reaction flux to the advection rate:

$$N_D = \frac{\ell M \bar{R}_d c_s}{v c_f} = \frac{\ell}{v}\frac{J_{tot}}{c_f} \tag{22}$$

where J_{tot} is the total reaction flux per unit volume fluid. Damköhler numbers have been defined in different ways for various uses; for diffusion-dominated transport a different form exists [*Boucher and Alves*, 1959]. Also, they can be used for any dimensionless concentration and are not restricted to isotope ratios.

In advective systems the value of the Péclet number is dictated by the dispersivity, and generally, the dispersion term is somewhat less important than the advection term. Pe can be estimated based on knowledge of the system, leaving the Damköhler number as the critical parameter, in the absence of mixing effects, that describes the evolution of isotope ratios along the flow path. The $[\bar{r}_d - r_f]$ term gives the degree of isotopic disequilibrium between solid and fluid at any position and time. As the fluid progresses and reacts with the rock, its isotope ratio tends toward that of the solid, and this term tends toward zero. The Damköhler number describes the rate at which the fluid equilibrates with the solid. For example, if rock composition and fluid concentration are constant over distance, and the effects of dispersion are neglected, isotopic disequilibrium will decay exponentially with distance traversed, with N_D as the exponential factor. This follows from the steady state solution of (21) for constant $\bar{r}_d$ and $D = 0$, which is plotted in Figure 2:

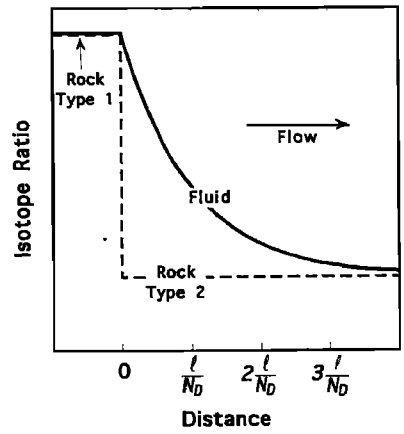

Figure 2. The evolution of an isotope ratio in a simple water-rock system as a function of distance. The solution is initially out of isotopic equilibrium at the rock type change ($x = 0$). Neglecting dispersion effects, and assuming the Damköhler number is constant, the disequilibrium decays by a factor of e for each distance ℓ/N_D traversed.

$$r(x') = \bar{r}_d + (r_{f,0} - \bar{r}_d)\exp(-N_D x') \tag{23}$$

where $r_{f,0}$ is the isotope ratio of the fluid at $x = 0$. For nonzero dispersion the solution has the same basic form, but includes Pe:

$$r(x') = \bar{r}_d + (r_{f,0} - \bar{r}_d)\exp\left(-\frac{2N_D}{1 + \left(1 + 4\frac{N_D}{Pe}\right)^{1/2}}x'\right) \tag{24}$$

This is close to (23) when Pe is large, but as Pe decreases, the distance over which the fluid equilibrates isotopically with the solid becomes longer as dispersive transport increases. In a typical case, where N_D is 1 and Pe is 10, the factor by which x' is multiplied in (24) is 0.9. In summary, for advective systems, solutions to (21) depend strongly on N_D and to a lesser extent on Pe. This reflects the importance of N_D as the critical parameter that describes the rate of reaction relative to advection and controls the distance over which isotope ratios evolve.

For fractionating isotopes the equations can be developed in a similar fashion. Equation (17) can be scaled to yield

$$\frac{\partial \delta_f}{\partial t'} = \frac{1}{Pe}\left(\frac{\partial^2 \delta_f}{\partial x'^2} + \frac{2}{c_f}\frac{\partial c_f}{\partial x'}\frac{\partial \delta_f}{\partial x'}\right) - \frac{\partial \delta_f}{\partial x'} + N_D\left[\bar{\delta}_d - \delta_f + \frac{\bar{R}_p}{\bar{R}_d}\bar{\Delta}\right] \tag{25}$$

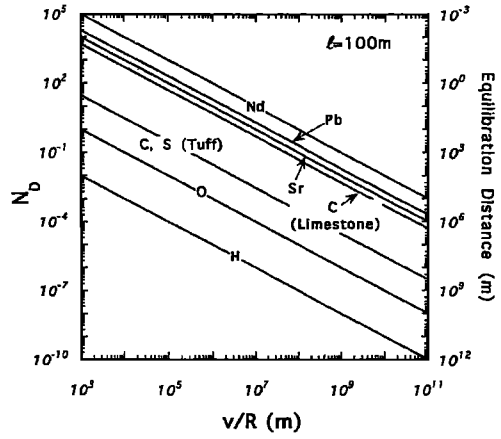

Figure 3. Estimated N_D values versus the ratio of fluid velocity to reaction rate, calculated from (22) for a system in which $M = 10$ and $\ell = 100$ m. The right-hand vertical axis gives the length scale for equilibration (i.e., ℓ/N_D). In a given system, N_D varies over several orders of magnitude between elements. Concentration data were taken from *Benson et al.* [1983] for waters in Yucca Mountain tuff aquifers. Other data are from *Drever* [1988] for granite and carbonate host rocks.

The steady state solution for a homogeneous solid and $D = 0$ can be expressed

$$\delta(x') = \left(\bar{\delta}_d + \frac{\bar{R}_p}{\bar{R}_d}\bar{\Delta}\right) + \left[\delta_{f,0} - \left(\bar{\delta}_d + \frac{\bar{R}_p}{\bar{R}_d}\bar{\Delta}\right)\right] \cdot \exp\,(-N_D x') \qquad (26)$$

This is very similar to (23), except that the equilibrium (large x') δ value is offset from $\bar{\delta}_d$. As in (23), the dissolution rate appears in N_D but the precipitation rate does not. The precipitation rate appears in (26) only as part of the term that determines the offset between the isotopic composition of the solid and that of the fluid at large x' (as stated above, for exchange reactions the dissolution and precipitation rates are actually the rates of cation diffusion out of and into the solid phases, respectively). In summary, for both nonfractionating and fractionating isotope pairs the key characteristic of the system that determines how rapidly the fluid takes on the isotopic signatures of successive segments of host rock is the Damköhler number as defined in (22).

Factors Determining the Damköhler Number

$N_D(\mathbf{x})$ is determined in part by the characteristics of the porous medium, but, perhaps more importantly, it varies strongly from one chemical element to another. The parameter that varies most strongly between elements is the ratio c_s/c_f, which varies over several orders of magnitude. In a given system the various elements will have a wide range of Damköhler numbers, depending on their solid/fluid partitioning (Figure 3). Those elements that are less abundant in the fluid relative to the solid have larger Damköhler numbers and are more susceptible to change via water-rock interaction, as a small amount of reaction produces a large flux from the solid relative to the concentration in the fluid. Generally, the rock-forming cations are strongly partitioned into the solid phases (e.g., Sr, $c_s/c_f = 10^3$–10^4 for Yucca Mountain groundwater). Other species have lower distribution coefficients (e.g., oxygen) and, as a result, will have smaller Damköhler numbers. In many cases, concentrations of dissolved elements are buffered by dissolution, precipitation, and exchange reactions so that c_s/c_f can be easily characterized or predicted. Solid-fluid partitioning also varies greatly between different types of rocks. For example, c_s/c_f for carbon in a limestone aquifer is high, while it is much lower in a silicate-dominated aquifer.

Other parameters that influence N_D are controlled primarily by the physical characteristics of the system and do not differ between elements. The average fluid velocity v and the solid-to-fluid mass ratio, M, are determined solely by hydraulic and physical parameters. The reaction rates, R_i, depend mostly on the minerals present and fluid conditions (pH, temperature, etc.), but in ion exchange and sorption reactions depend also on the element of interest. Some cations, like Sr, may exchange very rapidly with certain minerals, while other species may do so more slowly (e.g., Nd). In summary, N_D for a given species will vary from system to system, and as a function of position in a system, according to variations in velocity, porosity, and reaction rate. On the other hand, in a given fluid-rock system, N_D will take on a wide range of values for the various isotope ratios, according to solid-fluid partitioning of the chemical elements of interest and, to some extent, according to varying exchange rates.

Using the Damköhler number as a quantitative indication of the rate at which isotope ratios are altered by reaction, it becomes clear that the various isotope ratios contain different information about the physical and chemical properties of water-rock systems. At one extreme, when N_D is very small, the isotope ratio can be used as a "tracer"; distinctive "signatures" acquired at the recharge areas may be tracked to give information on flow paths. At the other extreme, if N_D is large, the fluid quickly attains isotopic equilibrium with successive rock masses and the "memory" of recharge areas is not retained. Finally, in an intermediate case, with $N_D \approx 1$, the approach to equilibrium will occur over the length scale of observation, and N_D may be calculated if appropriate measurements can be made. Thus the information contained in isotope ratio measurements may be related to recharge composition, to reactions with rock masses near the sampling points, or both. Because of the wide range of solid-fluid partitioning, in many systems a full range of isotope types from conservative to highly reaction-dominated may exist. For example, in a typical watershed, oxygen isotopes may serve as conservative tracers that help define the flow paths, while Sr isotopes may give information concerning water-rock interaction.

Response of the Fluid to Spatial Variations in the Solid

The examples above (e.g., Figure 2) illustrate the isotopic equilibration of the fluid phase with a homogeneous solid; here we consider the effects of periodic variations in rock composition along the flow path. Analytical solutions for heterogeneous solids are derived and then examined to explore the relationships between the variation in solid composition and the evolution of the fluid. One-dimensional, steady state, analytical solutions for sinusoidal variation of solid composition with distance are easily obtained; solutions for different wavelengths can then be added together to give solutions for more complex solid compositions. In this

way the fluid composition along the flow path can be calculated when the isotope ratio of the solid is an arbitrary function of distance, provided the Damköhler number is constant with distance. In the present context, however, this approach is useful in making more general observations.

For nonfractionating isotopes, if the isotope ratio of the reaction flux from the solid varies sinusoidally with distance,

$$\bar{r}_d(x') = A \sin\left(\frac{2\pi x'}{\lambda'}\right) \tag{27}$$

then (21) can be expressed (we assume, for simplicity, that c_f is constant over x and the second dispersion term vanishes)

$$\frac{\partial r_f}{\partial t'} = \frac{1}{Pe}\frac{\partial^2 r_f}{\partial x'^2} - \frac{\partial r_f}{\partial x'} + N_D\left[A \sin\left(\frac{2\pi x'}{\lambda'}\right) - r_f\right] \tag{28}$$

where A is the amplitude, and λ' is the dimensionless wavelength (λ divided by the length scale, l). The solution to this equation for the steady state case is a sine function, diminished in amplitude and shifted in phase:

$$r_f = \frac{A}{d} \sin\left(\frac{2\pi x'}{\lambda'} + \theta\right) \tag{29}$$

where d is the amplitude damping factor,

$$d = \left[\frac{(2\pi/\lambda')^2}{(N_D)^2} + \left(1 + \frac{(2\pi/\lambda')^2}{PeN_D}\right)^2\right]^{1/2} \tag{30}$$

and θ is the phase shift,

$$\theta = \tan^{-1}\left(\frac{2\pi/\lambda'}{N_D + \dfrac{(2\pi/\lambda')^2}{Pe}}\right) \tag{31}$$

Examination of (30) reveals that the amplitude of the fluid response depends on the relative sizes of the Damköhler number and the wavelength. If N_D is large relative to $2\pi/\lambda'$, the damping factor is small and the fluid closely mimics the spatial variation in the solid. If N_D is small relative to $2\pi/\lambda'$, the damping factor is large and the fluid responds little to the solid variation. For a given value of N_D the response in the fluid to short-wavelength variation in solid composition is more highly damped, while the fluid response to longer-wavelength variation is less damped and more closely mimics the solid composition. The solution for the fractionating isotope case is similar; the only difference is the introduction of a term that shifts the isotopic composition of the fluid.

For solid compositions that can be expressed as the sum of many sine components, the analytical solution can be obtained by adding the solutions for separate statements of (28) for the sine components. In Figure 4, solutions are plotted for a system where the isotope ratio of the reaction flux from the rock is

$$\bar{r}_d = \sin(2\pi x') + \frac{5}{3}\sin\left(\frac{2\pi x'}{5/3}\right) + 5\sin\left(\frac{2\pi x'}{5}\right) \tag{32}$$

The fluid compositions plotted are sums of three statements of (29) for the three sine components. For $N_D = 1$, it is clear that the fluid responds strongly to the longer-wavelength variation of the solid and responds only slightly to the shorter-wavelength variation. At higher N_D the fluid mimics the solid more closely, and shorter-wavelength variation appears in the fluid.

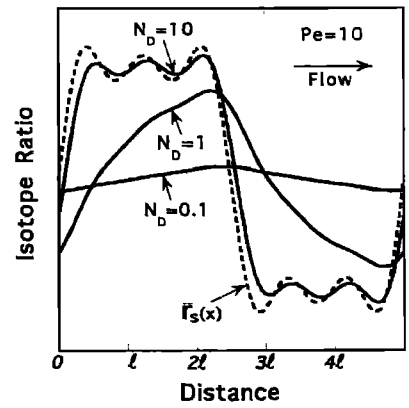

Figure 4. Analytical solutions for the isotope ratio of the fluid phase as it flows through a solid that has a spatially variable isotope ratio. The isotope ratio of the reaction flux (dashed line) as a function of distance is the sum of three sine functions, and is given in (32). Calculated fluid compositions are plotted for three values of N_D; Pe is fixed at 10. As N_D increases, the fluid shows greater response to short-wavelength variations in the solid.

In a natural system this relationship between N_D and the wavelength of variation in the fluid may be used to estimate the value of N_D. Qualitatively, if the fluid shows short-wavelength variation, N_D must be large. If the fluid shows only long-wavelength variation, then either N_D is small or only long-wavelength variation is present in the solid. This type of analysis can also be quantitative: If measurements of isotope ratios are made to find the amplitude and wavelength of variations in the fluid, and the wavelength and amplitude of spatial variation in the solid can be estimated for a given host rock, an estimate for N_D can be calculated using (30).

Applying the Model to Natural Systems

Equation (8) for nonfractionating isotope pairs, or (11) for fractionating isotope pairs, provides the model through which isotope measurements $r_f(\mathbf{x}, t)$ on fluids or fluid-deposited minerals can be related to the transport parameters $\mathbf{D}(\mathbf{x})$ and $\mathbf{v}(\mathbf{x})$, and the reaction parameters $M(\mathbf{x})$, $R_i(\mathbf{x})$, $r_i(\mathbf{x})$, $c_i(\mathbf{x})$, and $c_f(\mathbf{x})$. We emphasize that our approach does not require isotopic equilibrium between fluid and solid, as is commonly assumed in higher-temperature systems. Moreover, it is precisely the departure from equilibrium (i.e., the value of $[\bar{r}_d - r_f]$ in (21)) that gives the critical information. In analyzing data from advective systems where reaction plays a role, the Damköhler number is the fundamental parameter extracted from the data. Estimates of the Péclet number are needed for accurate interpretations, and mixing between distinct fluid masses may be important, as mixing effects may overwhelm reaction effects and may be the dominant source of spatial variation in some systems. However, mixing effects and reaction effects can potentially be separated if observations of isotope ratios of both high-N_D and low-N_D elements are available.

Observation of isotope ratio changes along a flow path, combined with knowledge of the isotope ratios of the solid,

can give a value of N_D, or possibly $N_D(\mathbf{x})$, and this is the basic form that the results take. Under ideal conditions, a value of N_D derived from an isotope tracer test (e.g., Sr isotopes) could be used directly in predicting future transport of the element of interest in the system (e.g., of ^{90}Sr). This predictive strategy could be expanded to include other elements involved in the same mineral reactions, after accounting for differences in the fluid-solid partitioning of the elements.

Values of the Damköhler number may be obtained using isotope data, but it is important to note that the values of the individual parameters that compose the Damköhler number are not directly obtained. Additional information must be given to obtain these. If some of the parameters are known or can be estimated, values for other less well constrained parameters within N_D can be calculated. Typically, the reaction rates and/or fluid velocity are the least well constrained, whereas the other parameters can be estimated easily. In a system that is well characterized hydrologically and petrologically, the groundwater velocity (v), the relative masses of solid and fluid (M), the concentration of the element of interest in the fluid (c_f), and the concentration and isotope ratio in the solid phases and fluid (c_i, r_i, c_f, r_f) may all be available. Since R_i, the reaction rates of the solid phases, are the only unknown quantities in N_D, these may be calculated. In the simple case where the solid is a single phase, there is no ambiguity, and R can be calculated directly using (22) [e.g., *Richter and DePaolo*, 1987, 1988; also F. Richter and Y. Liang, manuscript in preparation]. With multiple phases in the solid, the more strongly reacting phases may be identifiable, along with their reaction rates. In a situation where data on multiple isotope ratios are available, each with different values of c_i and c_f, it may be possible to solve simultaneously for the relative rates of multiple reactions.

If the flow field at a site is not well characterized, but the reaction flux from the rock can be estimated, information about the flow field may be extracted through application of the model. For example, if fluid in isotopic equilibrium with one rock type passes into an isotopically distinct rock mass, the fluid will evolve toward a new isotopic equilibrium at a rate dictated by the Damköhler number. Measurements of fluid isotope ratio can be used to observe this evolution, and, at least, give an indication of flow direction. More careful measurements can yield an estimate for N_D, which in combination with estimates of the reaction flux may constrain the groundwater velocity. Similarly, changes in the hydrologic regime with time can be detected by monitoring of isotope ratios.

Spatial variations in N_D may be used as a measure of variations in fluid velocity if it can be assumed that the reaction rate is spatially constant. For example, zones of unusually high hydraulic conductivity in otherwise homogeneous rock would have relatively low N_D values. Fluid migrating through a highly permeable zone would travel relatively long distances before attaining isotopic equilibrium with the host rock, while in zones with slower flow the equilibration distance would be smaller. Such a situation is illustrated in Figure 5. The transmissive middle layer has a lower N_D value than the surrounding rock, and this could easily be observed if the isotopic composition of the fluid were measured at various depths. It is important to note, however, that the relationship between N_D, which determines the equilibration distance along the flow path, and the transverse dispersivity, which controls mixing between the layers, is critical in determining the evolution of the fluid along the flow path.

Yucca Mountain Paleohydrology Investigations

Isotope data from secondary minerals at the proposed nuclear waste repository site at Yucca Mountain, Nevada, have been used to study the paleohydrology. We present here an analysis of some of these data based on the reaction-transport model presented above. A cross section of the geologic structure is given in Figure 1, showing the subhorizontally bedded silicic tuff units of the Yucca Mountain section. The proposed repository horizon is within the Topopah Springs unit, and the Calico Hills unit immediately below is notable for its high zeolite content. Mineralogical compositions are outlined in Figure 7. The hydrogeologic framework for the site has been investigated in detail, providing a physical and chemical characterization with which the system can be studied [cf., *Sinnock et al.*, 1987; *Narasimhan and Wang*, 1992; *Winograd*, 1974, 1975].

Strontium isotope ratios previously measured in calcite fracture fillings from deep drill cores [*Marshall et al.*, 1992] are the focus of the present study and are plotted in Figure 6. Uranium decay series analysis of similar calcite samples [*Szabo and Kyser*, 1990] has yielded 10 ages in the 26–310 ka range and four ages greater than the limit of the technique (400 ka); the veins thus apparently reflect relatively recent conditions. However, there is concern that sample heterogeneity may have affected these results, and work is in progress to refine these age dates (D. Vanamin, personal communication, 1993).

There is considerable scatter in the Sr isotope data, but

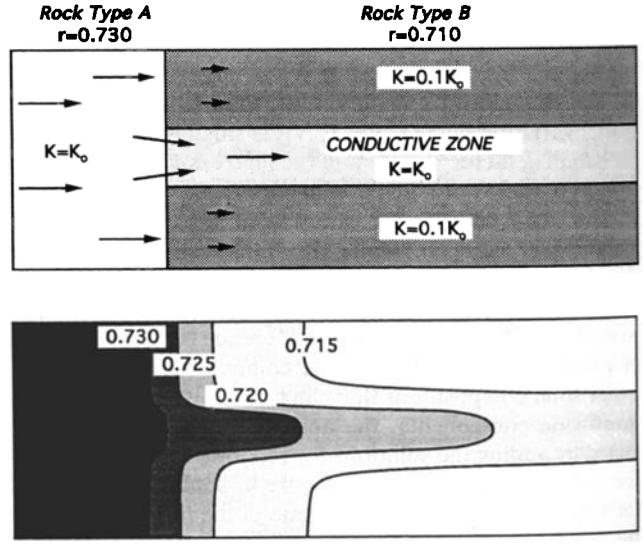

Figure 5. Isotopic evolution of waters flowing into an isotopically distinct rock mass. Reaction rates are assumed uniform throughout rock type B, and fluid is assumed to be in isotopic equilibrium with rock type A before contact with B. The Damköhler number is smaller in the more conductive zone where the fluid velocity is higher; this zone could be identified via isotope measurements because the fluid equilibrates with the new rock type over a longer distance.

this may be expected for data from multiple drill holes several kilometers apart. The data reveal a clear pattern (Figure 6); calcite samples from levels higher than 100 m above the modern water table have Sr isotope ratios distinctly higher than those measured in calcites from the saturated zone and similar to those in calcite deposits at the surface on Yucca Mountain. It has been proposed [*Marshall et al.*, 1992; *National Research Council*, 1992] that all of the vein calcite in the unsaturated zone was precipitated from downward percolating waters in a hydrologic regime similar to the present one; this implies that there is little likelihood of the repository's being flooded because of a higher water table in the future. However, scenarios have also been discussed [*National Research Council*, 1992] in which periodic rise of the water table could threaten the proposed repository, and in which the soil zone and vein calcites are interpreted as deposits formed from upwelling groundwater or in a paleo–saturated zone in a regime where the water table was higher than the modern level.

Initial interpretations of the data [*Marshall et al.*, 1992; *National Research Council*, 1992] emphasized that the analyzed unsaturated zone calcite veins could not be formed directly from saturated zone waters of present-day composition; these waters have distinctly lower Sr isotope ratios than the calcite. These studies concluded that the data support the hypothesis of a water table that has not risen more than 100 m above its present level. However, including water-rock interaction in the analysis may allow scenarios involving a higher paleo–water table to be consistent with the Sr isotope data from the drill core and surface carbonate deposits. As shown in Figure 7, the isotope ratio of the rock increases upward, and in the unsaturated zone is much higher than that of the saturated zone waters [*Peterman and Stuckless*, 1993]. If groundwater were to flow from the lower tuffs into the upper tuffs, as it passed through the rocks of the present-day unsaturated zone, it would react with the rocks and its Sr isotope ratio would increase, perhaps enough to produce the pattern seen in the calcite data. The effects of reaction may be great, despite the slow rates of reaction at near-surface temperatures; Sr concentrations are several orders of magnitude greater in the rock than in the fluid, and the Sr isotope ratio of the fluid is relatively susceptible to reaction effects. The question that follows naturally from this reasoning is whether or not the reaction-transport parameters required to duplicate the observed Sr isotope values in such a scenario are quantitatively consistent with what is known about the system at this time. We present here a first attempt at addressing this problem.

In addition to examining high–water table scenarios, we also examine the implications of assuming that the calcite veins formed under conditions similar to those existing today. One of the key features of the Yucca Mountain repository concept is the expected slow fluid migration through the unsaturated zone. At very low velocities, it can be conjectured that the Sr isotope ratio in the fluid would have ample opportunity to reach equilibrium with the rock. Inspection of the data (Figure 7) reveals that waters that formed the calcite were far from isotopic equilibrium with the rock. Evaluation of the significance of this disequilibrium requires a coupled reaction-transport model, and we have applied the model developed above to this task. Order-of-magnitude estimates for the transport and reaction parameters enabled extraction of information about the system from the isotopic data.

Application of the Model

The data set required to set up the model and analyze results was obtained from several sources. Whole rock Sr isotope ratios and Sr concentrations have been measured throughout the tuff section [*Peterman et al.*, 1991; *Spengler and Peterman*, 1991], and Sr isotope ratios in pedogenic carbonates found on the surface of Yucca Mountain are also known [*Marshall et al.*, 1991]. Groundwater Sr concentrations [*Benson et al.*, 1983], effective porosities for the Yucca Mountain tuff units [*Sinnock et al.*, 1987], and carbon 14 age dates on groundwater samples [*Benson and McKinley*, 1985; *White and Chuma*, 1987] enable estimation of other critical parameters of the system.

Incorporation of all of these data into an analysis of the interplay of transport processes, reaction rate, and changes in rock composition along the flow path was accomplished via numerical solution of the equations presented above. A one-dimensional model, (21), was used to approximate the system. The tuff units are relatively uniform along subhorizontal bedding planes (Figure 1), while isotopic variation across bedding is strong. In the simulations of vertical, unsaturated, flow across the bedding, the one-dimensional model is clearly appropriate. In other models, where flow is not directly across the bedding, the one-dimensional model is used as an approximation, and attention is focused on the component of solute transport across the bedding, (i.e., in a subvertical direction), under the assumption that the effects of sub-horizontal transport along bedding are of minimal importance. Thus the x axis in the model was oriented perpendicular to the bedding, in a nearly vertical direction. The equation was solved for steady state conditions, as no time series information is available for boundary conditions (the consequences of this assumption are discussed below). The rock composition was assumed to be invariant with respect to time, because of the slow rate at which the reactions alter the rock. The characteristic length scale for the system was set at 100 m, the distance over which the major isotopic contrast in the system occurs.

In the model the reactions responsible for governing the evolution of fluid isotope ratios are (l) dissolution of feldspar and (2) cation exchange with zeolites and clay minerals. Exchange reactions between Sr^{2+} adsorbed onto surfaces and Sr^{2+} in the fluid were ignored despite the rapid rate at which they occur; the adsorbed ions should be very close to isotopic equilibrium with the fluid. It is important to note that this is not the case in models of radionuclide transport, where a highly transient pulse of contrasting isotopic composition is attenuated largely by adsorption. Also, the reaction rate was assumed to be constant as a function of depth as a first-order approximation (although in one model, reaction was restricted to the Calico Hills unit only).

The Sr isotope ratio of the reaction flux from the rock at each node was set equal to an interpolated value of the whole rock ratio, and the magnitude of the Sr flux was assumed to be proportional to the whole rock Sr concentration. Sr concentration varies with depth in the section, so N_D varies with depth. For descriptive purposes the Damköhler number at the average Sr concentration of the section (124 ppm), designated N_D^0, is used below in discussing each simulation.

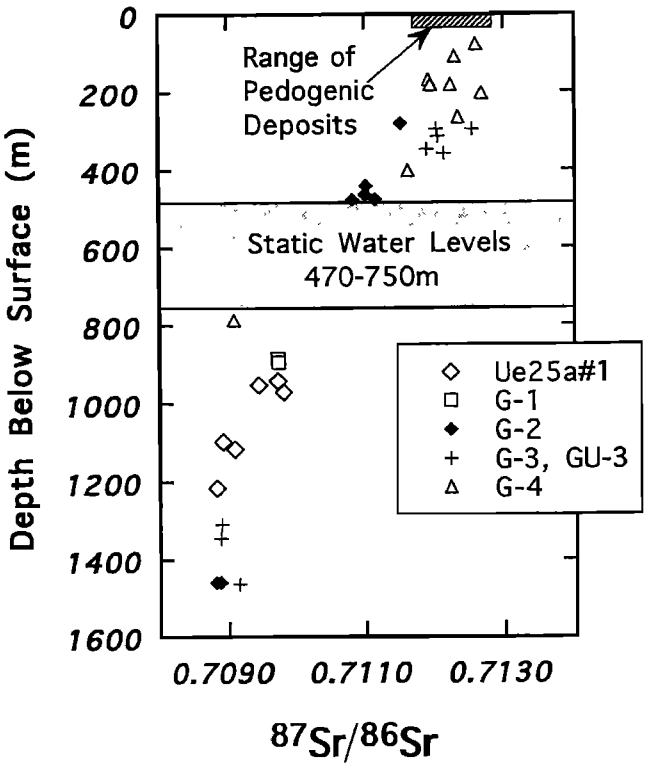

Figure 6. Ratio of ^{87}Sr to ^{86}Sr measured by *Marshall et al.* [1992] on calcite from vein fillings at Yucca Mountain. Drill hole numbers are given in the legend; the depth to the water table varies between holes. Calcite samples from above the present-day water table have higher $^{87}Sr/^{86}Sr$ than those below it.

The concentration of Sr in the fluid, c_f, was assumed to be constant throughout the section, though in nature, some variation would be expected.

The numerical modeling was used to find values of N_D^0 for which the modeled fluid fits the Sr isotope data from the vein calcites. Then, these N_D^0 values were combined with estimates of most of the parameters contained in N_D^0 to calculate values for the least well known parameter, the reaction rate. These values are the reaction rates required to fit the model to the data. The likelihood of each scenario was judged by comparing the required reaction rate to estimates of the actual reaction rate.

Model Scenarios

The first set of calculations, model 1, simulates modern conditions. The interval from the top of the Topopah Springs unit to the present depth of the water table (about 500 m below the top of the Topopah Springs unit) is considered, the rock is unsaturated, and fluid flow is downward. Modeling studies of unsaturated fluid flow in Yucca Mountain tuff [e.g., *Wang and Narasimhan*, 1985, 1990] suggest that transport is predominantly by porous flow through the matrix blocks, so the porous medium assumption implicit in (21) is justified. The Sr isotope ratio of the incoming solute at the top of the simulation was set equal to 0.7122, the average for pedogenic carbonates found on the surface of Yucca Mountain [*Marshall et al.*, 1991].

Higher paleo–water table conditions were simulated in two additional groups of calculations (models 2 and 3). In these scenarios, flow is either horizontal or upward. In the case of horizontal flow similar to that in the modern system, groundwater flows southeastward, based on hydraulic gradient, and the tuff layers dip eastward, so the water moves upsection (toward higher stratigraphic levels) as it flows. Thus the direction of flow in the model is upsection. The isotope ratio of the groundwater entering the model was set at 0.7090 so that the water was near isotopic equilibrium with the calcite veins deep below the modern water table. In model 2 the reaction rate was assumed constant over the entire modeled section. However, because the mineralogical composition of the tuffs varies between units (Figure 7), it is likely that the reaction rate is not constant with depth. The Calico Hills unit (330–450 m depth in the model section) is predominantly composed of zeolite minerals, though near the southern end of Yucca Mountain it is composed of glassy tuff [*Bish and Chipera*, 1989]. It is likely that rapid cation exchange or devitrification causes the reaction rate to be much greater in this unit than in other units. As an example of the effects of such heterogeneity, model 3 was constructed for the extreme case in which reaction occurs only in the Calico Hills unit (Figure 10). Finally, model 4 was constructed to examine the effects of changes in the Péclet number; it is similar to model 3 except that Pe was varied.

The Porous Medium Approximation for Fracture-Dominated Flow

In the high paleo–water table scenarios (models 2 and 3) the entire modeled section is saturated, and under these conditions, transport is dominated by fracture flow. Gener-

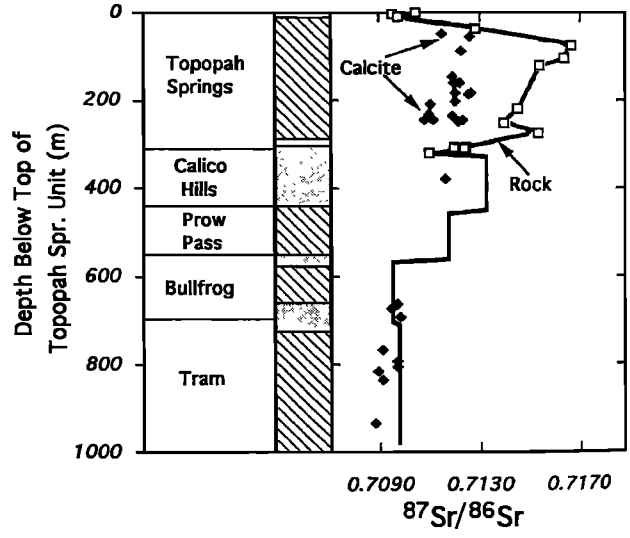

Figure 7. Whole rock $^{87}Sr/^{86}Sr$ plotted against depth below the top of the Topopah Springs unit. This stratigraphic depth scale enables comparison of the calcite with host rock. Values in the Topopah Springs unit are interpolated from *Peterman et al.* [1991] (data shown as open squares), while values in other units are from composite samples from each unit, as reported by *Spengler and Peterman* [1991]. The bar to the left of the graph gives the mineralogy as a function of depth: Lined intervals are devitrified tuff composed predominantly of quartz and alkali feldspar. Stippling indicates zeolitic intervals. Open intervals are vitric tuff. (The Calico Hills unit is vitric in some areas.)

ally, (21) applies only in porous media, but it can be used for fracture-matrix systems under some circumstances. If the diffusive communication between matrix blocks and fractures is strong relative to the reaction rate, then (21) is appropriate because all of the water in the matrix pores is involved in advective transport by virtue of its diffusive connection with the moving fracture water. In this case the fluid velocity used in the model is an effective parameter that describes the average velocity of the matrix water and fracture water combined. In the Yucca Mountain tuffs, the fracture density ranges from 5 per m^3 in the Calico Hills unit to 40 per m^3 in the densely welded core of the Topopah Springs unit [*Sinnock et al.*, 1987], implying that average fracture spacings are less than 1 m and are usually far smaller. Over these distances, and with the reaction rates expected for the system (discussed below), Sr isotope ratios in fractures can be shown to be effectively the same as those in the matrix blocks using a steady state, one-dimensional diffusion model. Thus for this range of fracture spacing, diffusion is fast enough to allow the porous medium approximation. It is important to note, however, that this is not the case for models of radionuclide migration, in which rapid sorption reactions are important.

Dispersivity and the *Pe* Values Used in the Models

Dispersivity values in large-scale systems are difficult to measure and are scale dependent. However, tracer tests in a variety of fractured rock settings give longitudinal dispersivities of the order of one-tenth the migration distance of the tracer [*Neretnieks*, 1985]. Thus in the models, where the isotopic contrast occurs over a distance of the order of 100 m, we estimate the mechanical dispersivity to be of the order of tens of meters. This gives a Peclet number of order 10. In the high–water table, horizontal flow model, dispersion in the direction of modeling is generated partially by transverse dispersion associated with the horizontal flow. However, transverse dispersivities appear to be at least an order of magnitude smaller than longitudinal dispersivities at both field and laboratory scales [*Domenico and Schwartz*, 1990] so this additional dispersion effect was ignored. The high–water table models (models 2 and 3) were thus calculated with $Pe = 10$. In model 1 the unsaturated flow is very slow, and the effects of ionic diffusion are substantial. Assuming an effective diffusion coefficient of 10^{-10} m^2/s and a dispersivity of 10 m, diffusion and mechanical dispersion are of roughly equal magnitude when the flow velocity is 10^{-11} m/s, or about 0.3 mm/yr. At the velocity considered in model 1 below, 0.1 mm/yr, diffusion effects are greater than mechanical dispersion effects and are probably about as strong as advective transport, so the Péclet number was decreased by an order of magnitude, to 1.

Modeling Results

In each calculation, (21) was solved numerically using a finite difference technique with a regular node spacing of 10 m. The numerical routine, which was verified against analytical solutions given by (24), calculated forward in time from an arbitrary starting configuration until a steady state was achieved. Results for a variety of N_D^0 values were calculated, and the range of values consistent with the calcite Sr isotope data was found for each scenario. These N_D^0 values were then used to assess the likelihood of the scenarios and the implications of the observed Sr isotope values, based on present knowledge of the water-rock system.

Results for model 1, the simulation of downward transport through the unsaturated zone (i.e., modern conditions), are presented in Figure 8. Calculations of Sr isotope ratio as a function of depth are plotted for $N_D^0 = 0.1$, 1, and 10. It is clear from Figure 8 that waters within the Sr isotope ratio range of the pedogenic carbonates could percolate downward to form calcite veins of the observed composition only if the effects of water-rock interaction were minimal. If N_D^0 were greater than 1, the Sr isotope ratio of the water would attain high values in the center of the Topopah Springs unit and this model would be inconsistent with the calcite data.

Results from models 2 and 3, for high–water table conditions, are presented in Figures 9 and 10. In model 2, N_D^0 was assumed constant over the entire vertical interval; the results for $N_D^0 = 0.2$ and 1.0 are given. As the water rises, it reacts with the rock and its isotope ratio increases. Values of N_D^0 in the range 0.2–1.0 are consistent with the calcite Sr isotope data . Results for model 3, the case where reaction is restricted to the Calico Hills unit, are given in Figure 10. N_D^0 values in the range of 1–5 in the Calico Hills unit are consistent with the Sr isotope data in this scenario.

In Figure 11, results from model 4 are presented. The model is similar to model 3, but lower Péclet numbers (Pe = 1, 0.1) are used, to examine the case where dispersion becomes the dominant vertical transport mechanism and to examine the sensitivity of the model to uncertainties in Pe.

Interpretation of Modeling Results

The N_D^0 values obtained for the model scenarios above express the rates of reaction, relative to advection rates, that are required to produce the observed Sr isotope pattern. These results embody the reaction-transport information extracted from the data, and we can interpret this information by combining it with other data from the system. The definition of the Damköhler number given in (22) contains a few other parameters in addition to the reaction rate and velocity, and these are easily estimated. The whole rock Sr concentration as a function of depth, $c_s(x)$, is known [*Peterman et al.*, 1991; *Spengler and Peterman*, 1991], and the average concentration is 124 ppm. The Sr concentration in the fluid, c_f, is estimated based on the average value (30 ppb) for the Yucca Mountain area [*Benson et al.*, 1983]. The solid/fluid mass ratio, M, is a readily calculated quantity: Average effective porosity for the Yucca Mountain tuff units is about 15% [*Sinnock et al.*, 1987], and assuming a solid phase density of 2.5 g/cm^3, M is about 14 for the saturated models. For the unsaturated models, M was increased to 20 to account for the fact that the porosity is not entirely occupied by water.

The two remaining parameters contained within N_D^0, the advection velocity and the reaction rate, have much greater uncertainties. The water velocity is scenario dependent and thus is estimated separately in the evaluation of each scenario below. The reaction rate, which is the least well constrained of all the parameters, was treated as an unknown. Using the values for N_D^0 obtained from the modeling above and estimates of v for each scenario, R values were calculated from (22) and are compiled in Table 1. These values are then evaluated for consistency with mineralogical data and kinetic constraints.

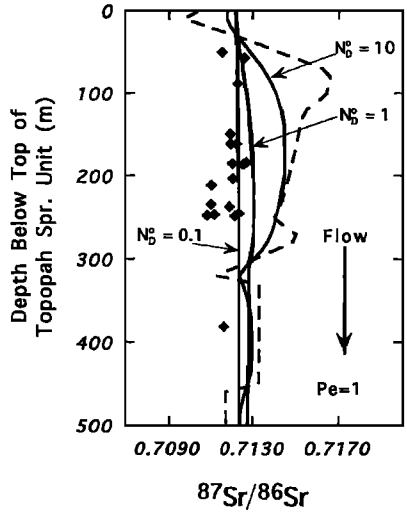

Figure 8. Ratio of ^{87}Sr to ^{86}Sr in the fluid, calculated using model 1, for descending water with water-rock interaction. In all four models the length scale, ℓ, is 100 m. Curves for three N_D values are plotted versus depth below the top of the Topopah Springs unit (solid lines). Fracture-filling calcites (solid diamonds) and whole rock (dashed line) are shown for comparison. The model is not consistent with the calcite data for N_D values greater than 1.

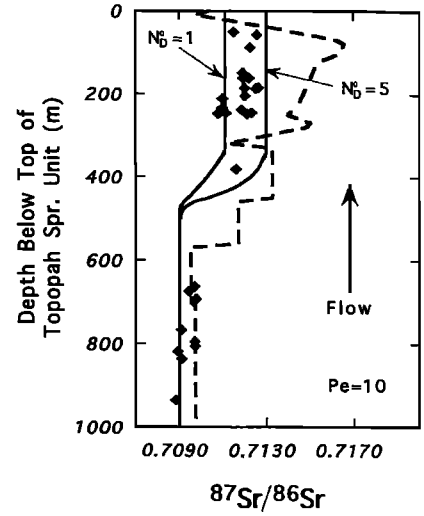

Figure 10. Ratio of ^{87}Sr to ^{86}Sr in the fluid, calculated using model 3, for upsection flow with N_D zero except in the Calico Hills unit. Curves for two N_D values are plotted versus depth below the top of the Topopah Springs unit (solid line) Vein-filling calcites (solid diamonds) and whole rock (dashed line) are shown for comparison. The model is consistent with the calcite data only for N_D values between 1 and 5.

Low-Water Table Scenarios

Model 1 simulates conditions similar to those at present, with downward, unsaturated flow. Diffuse porous flow in unsaturated silicic tuff is very slow, and models of downward flow velocities in the unsaturated zone at Yucca Mountain have constrained the velocity to less than 0.1 mm/yr [*Wang and Narasimhan*, 1985, 1990]. Model 1 is consistent with the calcite data only if N_D^0 is less than 1. Using $N_D^0 < 1$, a water velocity of 0.1 mm/yr, the values of M, c_s, and c_f given above, and (22), the reaction rate required by the model is $<1 \times 10^{-11}$/yr (1% of the solid dissolves per billion years).

Although the alkali feldspar that contains most of the Sr in the Topopah Springs unit [*Bish and Chipera*, 1989] is not highly unstable under ambient conditions, this reaction rate

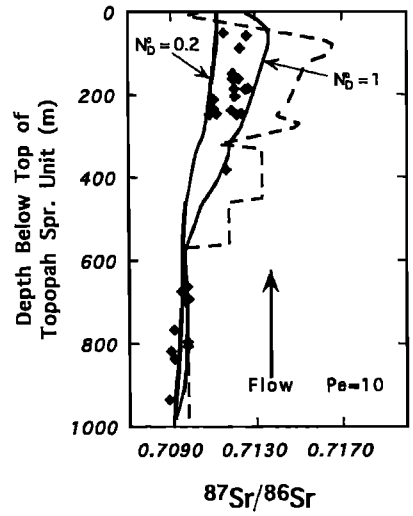

Figure 9. Ratio of ^{87}Sr to ^{86}Sr in the fluid, calculated using model 2, for upsection flow with N_D constant over depth. Curves for two N_D values are plotted versus depth below the top of the Topopah Springs unit (solid line). Vein-filling calcites (solid diamonds) and whole rock (dashed line) are shown for comparison. The model is consistent with the calcite data only for N_D values between 0.2 and 1.

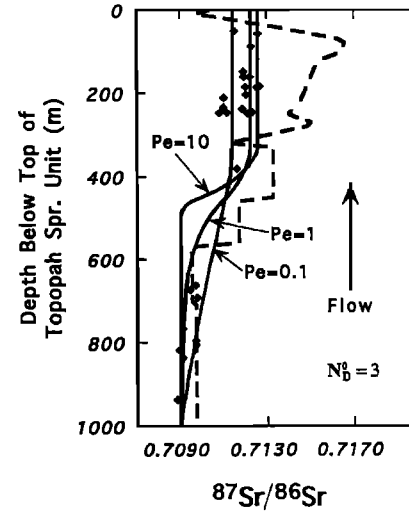

Figure 11. Ratio of ^{87}Sr to ^{86}Sr in the fluid, calculated using model 4, which is identical to model 3 except for the variation in Pe. The $Pe = 0.1$ model can be consistent with the calcite data, demonstrating that dominantly dispersive transport in the vertical direction could also give rise to the observed pattern. Also, the model results are not very sensitive to uncertainty in Pe. Changes in Pe do not change the basic result, and the reaction rate can be adjusted to compensate for them.

Table 1. Reaction Rates Required to Fit Models to the Calcite Sr Isotope Data

Scenario	N_D Range From Model	Estimated v, m/yr	Calculated R, yr^{-1}
Model 1: Downward flow	<1	1×10^{-4}	$<1 \times 10^{-11}$
Model 2: Horizontal flow	0.2–1	1	0.4×10^{-7} to 2×10^{-7}
Model 2: Fast upward flow	0.2–1	>10	$>0.4 \times 10^{-6}$ to 2×10^{-6}
Model 3: Horizontal flow, reaction in CH unit only*	1–5	1	2×10^{-7} to 9×10^{-7}
Model 3: Fast upward flow, reaction in CH unit only*	1–5	>10	$>2 \times 10^{-6}$ to 9×10^{-6}
Model 4: Dispersive transport, reaction in CH unit only*	3	0.1	5×10^{-9}

*CH, Calico Hills.

is extremely low and difficult to justify. The rock is porous, with about 10% effective porosity in the most thoroughly welded layers, and the grain size is fine, resulting in a very large surface area. Values of the order of 10^8 cm^2/L are reported for the Paintbrush tuff in Rainier Mesa on the Nevada Test Site [*Claasen and White*, 1979]. The Topopah Springs unit, which is the critical unit in this model, is 10 million years old and contains of the order of 1–5% low-temperature clay minerals [*Bish and Chipera*, 1989]. Assuming that these phases precipitated in response to dissolution of rock occurring at a constant rate since emplacement of the tuffs, a dissolution rate of about $1–5 \times 10^{-9}$/yr is implied. It is likely that some of this alteration occurred at accelerated rates while the tuffs were still cooling, so the modern reaction rate may be somewhat lower. We thus consider that this rate is a maximum rate for the system, but assert that the true rate is probably not nearly as low as 1×10^{-11}/yr.

If the reaction rate is indeed greater than 1×10^{-11}/yr, and if the vein calcites in the upper cluster precipitated under unsaturated, downward flow conditions, then the parent fluid must have been moving through the rock faster than 0.1 mm/yr. This is not allowable under steady state, unsaturated, porous flow conditions, but recent studies have suggested that "fast paths" exist whereby transient pulses of fluid may move rapidly through fractures without being imbibed into matrix pores [*Wang et al.*, 1993]. Environmental isotope data from Yucca Mountain also suggest that transport is spatially variable and, at least intermittently, much faster than previously estimated [*Yang*, 1992]. It is not possible to extend our model to this transient case, but in a qualitative sense, the observed vein calcite Sr isotope data are well explained by deposition of fracture-filling calcite from waters moving in a "fast path" mode.

Higher–Water Table Scenarios

The models for high–water table conditions may be applied to two distinct scenarios for the cause of the water table rise: In the first scenario, flow is predominantly horizontal, as at present, but with a higher water table (perhaps in response to increased recharge). In the second, groundwater rises beneath Yucca Mountain in response to some local driving force (we do not imply that such a scenario is hydrologically reasonable; we wish to examine the geochemical evidence here independently). The groundwater velocity in the first scenario can be constrained because of its similarity to the present-day system. As explained above, we have applied a porous medium model to a fracture-dominated system, and the velocity parameter in such a model is an effective velocity. The effective velocity is smaller than the fracture velocity because the matrix pore waters are linked to the fractures by diffusion. Fortunately, velocities calculated from carbon 14 age dates of groundwaters are also effective chemical transport velocities of the same type, and we use these as the best estimate available for the model. Carbon 14 ages from wells in the Yucca Mountain area [*Benson and McKinley*, 1985], corrected for acquisition of dead carbon after recharge [*White and Chuma*, 1987] and combined with the approximate distance to the recharge area, give regional velocities of the order of 10 m/yr. Well tests near Yucca Mountain have given permeability values that correspond to higher velocities [*Sinnock et al.*, 1987], but this is to be expected: The carbon 14 results reflect an effective fluid velocity (fracture flow plus diffusive communication with matrix fluid), while the physical tests relate to true fracture velocity. The appropriate value for the Sr transport model presented here is the carbon 14–based estimate. This is an order-of-magnitude estimate; there are uncertainties in the dating, and the local velocity may differ from this regional value according to varying potentiometric gradients and interformational variations in hydraulic conductivity.

In the case of a higher paleo–water table with subhorizontal flow similar to that in the present system, the water moves upsection as it flows. The component of flow in the modeled direction (perpendicular to bedding) depends on the apparent dip of the tuffs along the flow direction. That dip is approximately 5° [*Sinnock et al.*, 1987], and the resulting upsection velocity is of the order of 1 m/yr. In model 2, where the reaction rate is constant throughout the section (Figure 9), N_D^0 must be in the range 0.2–1.0 for the model to be consistent with the calcite data. With a velocity of 1 m/yr, and using the values of M, c_s, and c_f given above, the range of R calculated from (22) is $0.4–2 \times 10^{-7}$/yr. This is greater than the maximum reaction rate suggested above for the Topopah Springs unit, so this scenario is apparently not plausible.

While a uniform reaction rate model requires an unreasonably high rate in the Topopah Springs unit, the other units in the section, most notably the zeolite-rich Calico Hills unit, could have much higher reaction rates. The results of model 3 (Figure 10) suggest values of $N_D^0 = 1–5$ in the Calico Hills

unit and zero elsewhere are consistent with the Sr isotope data. For a velocity of 1 m/yr the required reaction rate would be about 2–9 $\times$ 10^{-7} per year, or 20–90% of the cations exchanged per million years. It is difficult to assess whether or not this is reasonable for the zeolitic or vitric layers, but the plausibility of this relatively high reaction rate is supported by the rapid exchange properties of zeolites and the high degree of alteration observed in the unit. In summary, while there are few kinetic constraints, it appears reasonable that the observed vein calcite could have been formed by groundwater that flowed upsection and reacted with the zeolites in the Calico Hills unit to attain higher Sr isotope ratios in the upper tuff units.

The results of model 4 (Figure 11) suggest that dispersive transport in the modeled direction, with very little advective transport, could also produce the observed Sr isotope pattern. The Pe = 0.1 case in Figure 11 corresponds to a situation where dispersion dominates over advection as the transport mechanism in the modeled direction. Such a situation might exist if the flow direction were parallel to bedding (as in the case where flow is in the due south direction), and transverse dispersion were the dominant transport mechanism in the direction perpendicular to bedding. The reader will note that the results are qualitatively similar regardless of the transport mechanism. Using the Pe = 0.1 case in Figure 11, we can calculate the reaction rate required to match the data for a reasonable estimate of the dispersion coefficient. If the transverse dispersivity of the system were 1 m and the horizontal fluid velocity were 10 m/yr, the dispersion coefficient would be 10 m^2/yr. Using this value, the Pe = 0.1 case in Figure 11 can be fit to the data with a reaction rate of about 5 $\times$ 10^{-9}/yr.

Actively upwelling waters, flowing upward in the vicinity of Yucca Mountain, could also produce the observed Sr isotope pattern. The velocity could be much greater than that estimated for the subhorizontal flow scenario above, and this would require greater reaction rates. This might be possible with rapid cation exchange in the zeolitic beds, and in general, the Sr isotope data cannot rule out a scenario where an actively upwelling groundwater flow system with the necessary Damköhler number existed and produced the observed calcite deposits.

Discussion

It is clear that the uncertainties in the Yucca Mountain models preclude their use in their current form for accurate forward modeling of the system. Nonetheless, given the constraints that were placed on the system parameters, we have gained some general insights into the effects of reaction on Sr isotope ratios in the system and can comment on the likelihood of various scenarios for the formation of the calcite veins, based on the limited information available.

The greatest obstacle to clear interpretation of the data is lack of knowledge about the reaction rates. In the analysis above, we used evidence from the rock itself to constrain the reaction rates, and we emphasize that such evidence may often be available when diagenetic processes are operating. It is also possible to use laboratory kinetic data to predict reaction rates, but several difficulties may be encountered. It is essential that the specific surface be known. If the solution is close to chemical equilibrium with the solid phases, the degree of disequilibrium must be known also, and this requires accurate chemical analysis of the waters. Such chemical data are not available for unsaturated zone waters at Yucca Mountain, and the saturated zone water analyses vary with location. However, assuming the waters are far from equilibrium, using the specific surface of the Paintbrush tuff as measured on the Nevada Test Site [*Claasen and White*, 1979], and using laboratory kinetic data for K-feldspar [*Lasaga*, 1984], the resulting reaction rate is of the order of 10^{-4}/yr, several orders of magnitude above what is physically reasonable based on the mineralogical composition of the rock. This discrepancy can be explained if the waters at Yucca Mountain are very close to chemical equilibrium with alkali feldspar, but on the other hand, kinetic studies in the field commonly measure rates a few orders of magnitude lower than predicted by the laboratory data [*Kenoyer and Bowser*, 1992; *Paces*, 1983; *Velbel*, 1985; *Holdren and Speyer*, 1987]. Overall, it appears that reaction rate information is difficult to obtain, both in the Yucca Mountain system and in general. This makes interpretation of flow patterns from groundwater Sr isotope data more difficult, but on the other hand, highlights the opportunity to use such data to improve our knowledge of reaction rates. In many modern systems, flow velocities can be predicted or measured to an order of magnitude or better, and under good conditions, isotope data could be used to derive reaction rates to similar degrees of precision.

Compared to the uncertainty in the reaction rate and velocity parameters, other uncertainties in the Yucca Mountain model are relatively minor. M, $c_s(x)$, $r_s(x)$, and c_f are all relatively well known, and changing any one of these parameters simply shifts the required reaction rates by the same factor. The estimates of the Péclet number used in the models are subject to substantial uncertainty, but generally the effects of changes in Pe are small or can be offset by changing the reaction rate slightly. In Figure 11 a comparison of results at three different Péclet numbers is shown. Generally, the results change little regardless of whether transport is dominantly advective (Pe = 10) or advective and dispersive (Pe = 1). The basic effect of increasing dispersion is that the overall transport rate increases. If dispersion has been underestimated in the models, this can be compensated for by increasing the reaction rate.

Model Assumptions

In the models the bulk rock isotopic ratio was used as an estimate for the isotopic ratio of the reaction flux. This may lead to some inaccuracy, because the isotope ratios of the solid phases vary according to their concentrations of Rb relative to Sr. In some settings, minerals with a wide range of isotope ratios may react at contrasting rates, giving a net reaction flux with an isotope ratio that is unrelated to the average of the reactants [*Bullen and Kendall*, 1993]. However, in the Yucca Mountain units, this is probably not the case. In the devitrified tuff units the mineralogy is dominated by alkali feldspar and quartz, and other minerals such as plagioclase and biotite occur only in trace amounts. High reaction rates would be required for the minor phases to dominate the reaction flux, and under such conditions, these phases would be effectively gone after 10^7 years of reaction since emplacement of the tuffs. Similarly, the zeolitic units are dominated by two zeolite minerals, clinoptilolite and mordenite, that exchange cations rapidly, so it is difficult to envision a minor phase dominating the reaction flux.

The steady state assumption in the models may create some inaccuracy in the low–water table scenario, model 1. Because of the slow flow rates, the time required to reach a steady state with respect to chemical transport in such a system is of the order of millions of years. Accordingly, changes in flow rate with time (e.g., in response to climate fluctuations) could cause nonsteady state effects, but these fluctuations should average out with time and the results should be similar to the steady state model. Alternatively, if the natural system has undergone major changes over the last million years, then there may be some "memory" of prior conditions that is not accounted for in our model. This effect could be significant, but the only clear possibility for such prior conditions would be saturation and faster flow. Thus the interpretation of model 1 assumes that the water table elevation has been stable for at least a million years.

Another inaccuracy arises if the porous medium approximation breaks down for the fracture-dominated saturated flow models (2 and 3). It is known that irregularities in fractures lead to channeling of flow [*Dykhuizen*, 1992; *Neretnieks*, 1985], which tends to decrease the surface area of flowing fluid in contact with matrix blocks. Also, interconnection between fractures may be poor [*Neretnieks*, 1985], and the effective fracture spacing may be much greater than the actual spacing. If these effects are large, they could be accounted for, to first order, by considering some fraction of the matrix volume inaccessible. This would have the effect of decreasing the amount of rock participating in the reaction, giving an effective reaction rate that is smaller than the actual reaction rate. Accordingly, the reaction rates might be adjusted to higher values if these effects are found to be significant. However, the most important rock unit in our analysis, the Calico Hills unit, is less fracture-dominated than the other units, and we consider the values arrived at above for model 3 reliable.

Despite uncertainty in the reaction rate and other parameters in the system, the constraints that do exist have allowed us to draw some conclusions about the system. Models 3 and 4, high–water table models, are capable of adequately reproducing the calcite vein Sr isotope data, based on the assumption that Sr exchange between zeolites and water and dissolution of glass are fast relative to dissolution of feldspar. Model 1, the low–water table model, is not capable of reproducing the data except at a reaction rate that we assert is unlikely in view of the observed smectite alteration in the Topopah Springs unit. The fast path scenario is the simplest explanation for the isotopic disequilibrium between the vein calcite and the host rock for low–water table scenarios.

Yucca Mountain Stable Isotope Data

Oxygen and carbon isotope data have also been gathered for vein calcites at Yucca Mountain. We have not explicitly analyzed those data, because reaction effects are probably negligible over the distances modeled in this study. For both oxygen and carbon the ratio of the concentration in the rock to that in the fluid is much lower than that for strontium. As a result, a given rate of reaction produces a much smaller effect on the carbon and oxygen isotope composition than on the Sr isotope ratio. For example, in Figure 9 the Sr isotope ratio changes substantially over about 200 m. In the same system the Damköhler number for oxygen would be about 4000 times smaller, and no substantial reaction effects would be expected. Thus we conclude that in this case, reaction effects need not be considered in the analysis of the carbon and oxygen isotopes. However, the reader will note that oxygen and carbon isotopes fractionate, and analysis of such data requires models that account for temperature variations and isotopic fractionation associated with evaporation, biological activity, liquid-vapor exchange, and vapor phase diffusion [*Quade and Cerling*, 1990].

Summary and Conclusions

The mathematical model developed here describes the evolution of isotope ratios in waters flowing through reactive media. It simulates the interplay of fluid-rock reaction and transport by advection and dispersion and is useful for interpreting measurements of isotope ratios in groundwater or groundwater-deposited minerals. The distance over which groundwater equilibrates isotopically with its host rock can be expressed using a Damköhler number, N_D, which controls the rate of evolution of groundwater isotope ratios. When water-rock interaction dominates the evolution of the groundwater composition, N_D is the key to interpreting the spatial and temporal patterns observed in data from arrays of wells or other sampling points. Despite the slow rate at which reactions occur in low-temperature systems, concentrations of many elements of interest in the groundwater are orders of magnitude smaller than those in the rock, and accordingly, a small reaction flux from the rock has a magnified effect on isotope ratios in the water. In other cases, flow paths are long (hundreds of kilometers) and the rock more reactive (e.g., limestone), so there may be substantial effects even for elements like oxygen and carbon. At temperatures well above 25°C, reaction rates are higher, Damköhler numbers increase, and virtually all dissolved elements are affected by reaction with rock.

Analysis of Sr isotopic data from Yucca Mountain using our model yields new interpretations of the data. Because of the effects of water-rock interaction, the Sr isotope ratios in calcite fracture fillings do not provide conclusive evidence either for or against past high–water table conditions. We do not argue in favor of a higher paleo–water table; the analysis published by the *National Research Council* [1992] provides several lines of reasoning against this scenario. We conclude here only that one of these is not conclusive because of water-rock interaction effects that were not considered in earlier studies. However, if it is hypothesized that the water table has been close to its current elevation during the formation of the calcite deposits, information regarding transport in the modern Yucca Mountain water-rock system can be extracted from the Sr isotope data. If it is assumed that at least some of the calcite veins formed under unsaturated conditions, the observed calcite Sr isotope pattern could not be produced during slow, matrix-dominated flow, barring an exceptionally low reaction rate. This conclusion is consistent with other studies suggesting the existence of "fast paths" through which solutions move rapidly in the unsaturated zone.

This application of the model highlights several aspects of the use of isotope data in groundwater studies. Many isotope ratios, and especially Sr, may be influenced by reaction effects; estimates of the Damköhler number serve as a guide in deciding when they are important. In some cases, reaction effects may complicate the interpretation of isotopes as

tracers, but in other cases isotope data still have value as indicators of flow velocity and/or direction. Reaction rates are often not well known. This inhibits forward modeling of reaction effects, but presents an opportunity to further the understanding of reaction rates using groundwater isotope measurements.

Notation

c_f, c_s concentration of a chemical species in the fluid phase and bulk solid, respectively (mass per unit volume fluid).

c_i concentration of a chemical species in the solid phase participating in the ith reaction.

$c_{2,f}$ concentration of the denominator isotope in the fluid phase (similar notation used for the concentration of the denominator isotope in the solid phases and bulk solid).

d damping factor; amplitude of fluid isotopic response divided by amplitude of solid variation.

$\mathbf{D}$ dispersion tensor.

J_i mass of the chemical element delivered to a unit volume of fluid by the ith reaction per unit time.

J_{tot} total mass of the chemical element delivered to a unit volume of fluid by all reactions per unit time.

ℓ length scale of the system.

M ratio of solid mass to fluid mass in a given volume.

N_D Damköhler number, a dimensionless quantity defined in (22).

N_D^0 Damköhler number corresponding to the average Sr concentration in the modeled Yucca Mountain rock section, equal to 124 ppm.

Pe Péclet number, equal to $v\ell/D$.

r_f, r_s isotope ratio in the fluid phase and in the bulk solid, respectively.

r_i isotope ratio of the solid phase participating in the ith reaction.

$\bar{r}_d$ isotope ratio of the flux from all dissolution reactions combined (see (15)).

R_i reaction rate of the ith reaction, expressed as the fraction of the solid phase dissolved per year or as the fraction of ions exchanged per year.

$\bar{R}_d$ combined dissolution rate, a weighted average of all dissolution rates (see (16)).

$\bar{R}_p$ combined precipitation rate, a weighted average of all precipitation rates (see (16)).

T temperature.

$\mathbf{v}$ average pore velocity of the fluid.

W_i mass of a particular solid phase per unit mass total solid; refers to the phase participating in the ith reaction.

$\alpha_j(T)$ isotope fractionation factor; the isotope ratio of the solid precipitated in the jth reaction divided by the isotope ratio in the fluid.

δ "delta notation"; per mil deviation of an isotope ratio from a standard value (subscript notation is the same as with isotope ratios).

$\bar{\delta}_d$ delta value of the flux from all dissolution reactions combined (see (15)).

$\Delta_j(T)$ difference between the δ value of the solid precipitated in the jth reaction and the δ value in the fluid phase.

ϕ effective porosity.

ρ_s bulk density of the solid (mass per unit volume solid).

ρ_f density of the fluid (mass per unit volume fluid).

Acknowledgments. This work was supported by the Director, Office of Energy Research, Office of Basic Energy Sciences, Engineering and Geosciences Division of the U.S. Department of Energy under contract DE-AC03-76SF00098. The manuscript was significantly improved through the recommendations of T. N. Narasimhan at Berkeley and three anonymous reviewers.

References

Banner, J. L., G. J. Wasserburg, P. F. Dobson, A. B. Carpenter, and C. H. Moore, Isotopic and trace element constraints on the origin and evolution of saline groundwaters from central Missouri, *Geochim. Cosmochim. Acta*, *53*, 383–398, 1989.

Benson, L. V., and P. W. McKinley, Chemical composition of ground water in the Yucca Mountain area, Nevada, *U.S. Geol. Surv. Open File Rep.*, *85-484*, 1985.

Benson, L. V., R. K. Robison, R. K. Blakennagel, and A. E. Ogard, Chemical composition of ground water and the locations of permeable zones in the Yucca Mountain area, Nevada, *U.S. Geol. Surv. Open File Rep.*, *83-854*, 1983.

Bish, D. L., and S. J. Chipera, Revised mineralogical summary of Yucca Mountain, Nevada, *Rep. LA-11497-MS*, Los Alamos Natl. Lab., Los Alamos, N. M., 1989.

Blattner, P., and K. R. Lassey, Stable-isotope exchange fronts, Damköhler numbers, and fluid to rock ratios, *Chem. Geol.*, *78*, 381–392, 1989.

Bottomley, D. J., and J. Veizer, The nature of groundwater flow in fractured rock: Evidence from the isotopic and chemical evolution of recrystallized fracture calcites from the Canadian Precambrian shield, *Geochim. Cosmochim. Acta*, *56*, 369–388, 1992.

Boucher, D. F., and G. E. Alves, Dimensionless numbers for fluid mechanics, heat transfer, mass transfer, and chemical reaction, *Chem. Eng. Progress*, *55*, 55–64, 1959.

Bullen, T. D., and C. Kendall, $^{87}Sr/^{86}Sr$ and $\delta^{13}C$ as tracers of interstream and intrastorm variations in water flow paths, Catoctin Mountain, Md. (abstract), *Eos Trans. AGU*, *72*(44), Fall Meeting suppl., 218, 1991.

Bullen, T. D., and C. Kendall, The natural variability of weathering input in a sandy silicate aquifer: Evidence from Sr isotopes in groundwaters and experimental extracts (abstract), *Eos Trans. AGU*, *74*(43), Fall Meeting suppl., 281, 1993.

Claasen, H. C., and A. F. White, Application of geochemical kinetic data to groundwater systems, in *Chemical Modeling in Aqueous Systems: Speciation, Sorption, Solubility and Kinetics*, edited by E. A. Jenne, pp. 771–793, American Chemical Society, Washington D. C., 1979.

Criss, R. E., R. T. Gregory, and H. P. Taylor Jr., Kinetic theory of oxygen isotope exchange between minerals and water, *Geochim. Cosmochim. Acta*, *51*, 1099–1108, 1987.

Domenico, P. A., and F. W. Schwartz, *Physical and Chemical Hydrogeology*, 824 pp., John Wiley, New York, 1990.

Drever, J. I., *The Geochemistry of Natural Waters*, 437 pp., Prentice-Hall, Englewood Cliffs, N. J., 1988.

Dykhuizen, R. C., Diffusive matrix fracture coupling including the effects of flow channeling, *Water Resour. Res.*, *28*, 2447–2450, 1992.

Holdren, G. R., Jr., and P. M. Speyer, Reaction rate–surface area relationships during early stages of weathering, II, Data on eight additional feldspars, *Geochim Cosmochim. Acta*, *51*, 2311–2318, 1987.

Kennedy, V. C., C. Kendall, G. W. Zellweger, T. A. Wyerman, and R. J. Avanzino, Determination of the components of stormflow using water chemistry and environmental isotopes, Mattole River basin, California, *J. Hydrol.*, *84*, 107–140, 1986.

Kenoyer, G. J., and C. J. Bowser, Groundwater chemical evolution in a sandy silicate aquifer in northern Wisconsin, 2, Reaction modeling, *Water Resour. Res.*, *28*, 591–600, 1992.

Lasaga, A. C., Chemical kinetics of water-rock interactions, *J. Geophys. Res.*, *89*(B6), 4009–4025, 1984.

Lassey, K. R., and P. Blattner, Kinetically controlled oxygen isotope exchange between fluid and rock in one-dimensional advective flow, *Geochim. Cosmochim. Acta*, *52*, 2169–2175, 1988.

Ludwig, K. R., Z. E. Peterman, K. R. Simmons, and E. D. Gutentag, $^{234}U/^{238}U$ as a ground-water tracer, SW Nevada- SE California, in *High-Level Radioactive Waste Management, Proceedings of the Fourth International Conference, Las Vegas*, pp. 1567–1572, American Nuclear Society, La Grange Park, Ill., 1993.

Marshall, B. D., Z. E. Peterman, K. Futa, and J. S. Stuckless, Strontium isotopes in carbonate deposits at Crater Flat, Nevada, in *High-Level Radioactive Waste Management, Proceedings of the Second International Conference, Las Vegas*, pp. 1423–1428, American Nuclear Society, La Grange Park, Ill., 1991.

Marshall, B. D., J. F. Whelan, Z. E. Peterman, K. Futa, S. A. Mahan, and J. S. Stuckless, Isotopic studies of fracture coatings at Yucca Mountain, Nevada, USA, in *Proceedings, Seventh Water-Rock Interaction Symposium, Park City, UT*, edited by Y. K. Kharaka and A. S. Maest, pp. 737–740, A. A. Balkema, Rotterdam, Netherlands, 1992.

McDonnell, J. J., M. Bonell, M. K. Stewart, and A. J. Pearce, Deuterium variations in storm rainfall: Implications for stream hydrograph separation, *Water Resour. Res.*, *26*, 455–458, 1990.

McNutt, R. H., S. K. Frape, and P. Dollar, Strontium, oxygen, and hydrogen isotopic composition of brines, Michigan and Appalachian Basins, Ontario and Michigan, *Appl. Geochem.*, *2*, 495–505, 1987.

Musgrove, M., and J. L. Banner, Regional ground-water mixing and the origin of saline fluids: Midcontinent, United States, *Science*, *259*, 1877–1882, 1993.

Narasimhan, T. N., and J. S. Y. Wang, Conceptual, experimental, and computational approaches to support performance assessment of hydrology and chemical transport at Yucca Mountain, *Rep. SAND89-7018*, 111 pp., Sandia Natl. Lab., Albuquerque, N. M., 1992.

National Research Council, *Ground Water at Yucca Mountain: How High Can It Rise?*, 231 pp., National Academy Press, Washington, D. C., 1992.

Neretnieks, I., Transport in fractured rocks, paper presented at 17th International Congress on Hydrogeology of Rocks of Low Permeability, Int. Assoc. of Hydrogeol., Tucson, Ariz., Jan. 7–12, 1985.

Paces, J. B., E. M. Taylor, and C. Bush, Late Quaternary history and uranium isotopic compositions of ground water discharge deposits, Crater Flat, Nevada, in *High-Level Radioactive Waste Management, Proceedings of the Fourth International Conference, Las Vegas*, pp. 1573–1580, American Nuclear Society, La Grange Park, Ill., 1993.

Paces, T., Rate constants of dissolution derived from the measurements of mass balance in hydrological catchments, *Geochim. Cosmochim. Acta*, *47*, 1855–1863, 1983.

Peterman, Z. E., and J. S. Stuckless, Isotopic evidence of complex ground-water flow at Yucca Mountain, Nevada, USA, in *High-Level Radioactive Waste Management, Proceedings of the Fourth International Conference, Las Vegas*, pp. 1559–1566, American Nuclear Society, La Grange Park, Ill., 1993.

Peterman, Z. E., R. W. Spengler, K. Futa, B. D. Marshall, and S. A. Mahan, Assessing the natural performance of felsic tuffs using the Rb-Sr and Sm-Nd systems—A study of the altered zone in the Topopah Spring member, Paintbrush Tuff, Yucca Mountain, Nevada, in *Mater. Res. Soc. Symp. Proc.*, *212*, 687–694, 1991.

Quade, J., and T. E. Cerling, Stable isotope evidence for a pedogenic origin of carbonates in trench 14 near Yucca Mountain, Nevada, *Science*, *250*, 1549–1552, 1990.

Richter, F., and D. J. DePaolo, Numerical models for diagenesis and the Neogene Sr isotopic evolution of seawater from DSDP Site 590B, *Earth Planet. Sci. Lett.*, *83*, 27–38, 1987.

Richter, F., and D. J. DePaolo, Diagenesis and Sr isotopic evolution of seawater using data from DSDP 590B and 575, *Earth Planet. Sci. Lett.*, *90*, 382–394, 1988.

Schrag, D. P., D. J. DePaolo, and F. M. Richter, Oxygen isotope exchange in a two-layer model of oceanic crust, *Earth Planet. Sci. Lett.*, *111*, 305–317, 1992.

Shemesh, A., H. Ron, Y. Erel, Y. Kolodny, and A. Nur, Isotopic composition of vein calcite and its fluid inclusions: Implication to paleohydrological systems, tectonic events and vein formation processes, *Chem. Geol.*, *94*, 307–314, 1992.

Sinnock, S., Y. T. Lin, and J. T. Brannen, Preliminary bounds on the expected postclosure performance of the Yucca Mountain repository site, southern Nevada, *J. Geophys. Res.*, *92*, 7820–7842, 1987.

Sklash, M. G., Environmental isotope studies of storm and snowmelt runoff generation, in *Surface and Subsurface Processes in Hydrology*, edited by M. G. Anderson and T. P. Burt, pp. 401–435, John Wiley, New York, 1990.

Spengler, R. W., and Z. E. Peterman, Distribution of rubidium, strontium, and zirconium in tuff from two deep coreholes at Yucca Mountain Nevada, in *High-Level Radioactive Waste Management, Proceedings of the Second International Conference, Las Vegas*, pp. 1410–1415, American Nuclear Society, La Grange Park, Ill., 1991.

Stuckless, J. S., J. F. Whelan, and W. C. Steinkampf, Isotopic discontinuities in ground water beneath Yucca Mountain, Nevada, in *High-Level Radioactive Waste Management, Proceedings of the Second International Conference, Las Vegas*, pp. 1410–1415, American Nuclear Society, La Grange Park, Ill., 1991.

Stueber, A. M., L. M. Walter, T. J. Huston, and P. Pushkar, Formation water from Mississippian-Pennsylvanian reservoirs, Illinois basin, USA: Chemical and isotopic constraints on evolution and migration, *Geochim. Cosmochim. Acta*, *57*, 763–784, 1993.

Szabo, B. J., and T. K. Kyser, Ages and stable-isotope compositions of secondary calcite and opal in drill cores from Tertiary volcanic rocks of the Yucca Mountain area, Nevada, *Geol. Soc. Am. Bull.*, *102*, 1714–1719, 1990.

Velbel, M. A., Geochemical mass balances and weathering rates in forested watersheds of the southern Blue Ridge, *Am. J. Sci.*, *285*, 904–930, 1985.

Wang, J. S. Y., and T. N. Narasimhan, Hydrologic mechanisms governing fluid flow in a partially saturated, fractured, porous medium, *Water Resour. Res.*, *21*, 1861–1874, 1985.

Wang, J. S. Y., and T. N. Narasimhan, Fluid flow in partially saturated, welded-nonwelded tuff units, *Geoderma*, *46*, 155–168, 1990.

Wang, J. S. Y., N. G. W. Cook, H. A. Wollenberg, C. L. Carnahan, I. Javandel, and C. F. Tsang, Geohydrologic data and models of Rainier Mesa and their implications to Yucca Mountain, in *High-Level Radioactive Waste Management, Proceedings of the Fourth International Conference, Las Vegas*, pp. 675–681, American Nuclear Society, La Grange Park, Ill., 1993.

Whelan, J. F., and J. S. Stuckless, Paleohydrologic implication of the stable isotopic composition of secondary calcite within the Tertiary volcanic rocks of Yucca Mountain, Nevada, in *High-Level Radioactive Waste Management, Proceedings of the Third International Conference, Las Vegas*, pp. 1572–1581, American Nuclear Society, La Grange Park, Ill., 1992.

White, A. F., and N. J. Chuma, Carbon and isotopic mass balance models of Oasis Valley–Fortymile Canyon groundwater basin, southern Nevada, *Water Resour. Res.*, *23*, 571–582, 1987.

Wigley, T. M. L., L. N. Plummer, and F. J. Pearson, Mass transfer and carbon isotope evolution in natural water systems, *Geochim. Cosmochim. Acta*, *42*, 1117–1139, 1978.

Winograd, I. J., Radioactive waste storage in the arid zone, *Eos Trans. AGU*, *55*, 884–894, 1974.

Winograd, I. J., Hydrogeologic and hydrogeochemical framework, south-central Great Basin, Nevada-California, with special reference to the Nevada Test Site, *U.S. Geol. Surv. Prof. Pap.*, *712C*, 126 pp., 1975.

Yang, I. C., Flow and transport through unsaturated rock: Data from two test holes, Yucca Mountain, Nevada, in *High-Level Radioactive Waste Management, Proceedings of the Third International Conference, Las Vegas*, pp. 732–737, American Nuclear Society, La Grange Park, Ill., 1992.

D. J. DePaolo and T. M. Johnson, Berkeley Center for Isotope Geochemistry, Department of Geology and Geophysics, University of California, Berkeley, CA 94720.

(Received August 3, 1993; revised January 10, 1994; accepted January 17, 1994.)